IMPaCT
EPSRC Centre for Doctoral Training in Innovative Metal Processing (IMPaCT)

Effects of welding parameters on sigma phase precipitation in 25Cr-5Ni-1Mo-2.5Cu-1Mn-0.18N duplex stainless steel

K. Yamada[1*], B. Holmes[2], K. Sotoudeh[2], H.B. Dong[1]
[1]University of Leicester, Leicester, LE1 7RH, UK [2]TWI Ltd, Cambridge, CB21 6AL, *ky77@leicester,.ac.uk

Introduction

Duplex stainless steels (DSSs) have been exploited by a wide range of industrial sectors for many years because of their mechanical properties and corrosion resistance. Whilst DSSs have excellent properties, **they are vulnerable to precipitate sigma phase during welding**, specially around the sigma phase precipitation temperature range 600-900°C.

New grade of duplex stainless steel UNS S82551 (25Cr-5Ni-1Mo-2.5Cu-0.18N) has been developed to achieve lower material cost than UNS S31803 (22Cr-5Ni-3Mo) and UNS S32750 (25Cr-7Ni-4Mo) by decreasing Mo content, which can be utilised in the as-welded condition in slightly sour condition[1-3].

<A new Steel - UNS S82551>

25Cr-5Ni-1Mo-1Mn-2.5Cu-0.2N (mass%)

Material	UNS No.	Chemical Composition (mass%)									Yield strength (MPa)
		C	Cr	Ni	Mo	W	Cu	Ti	N	PREW	
New DSS (DP25U)	S82551	max. 0.03	24.0 - 26.0	4.5 - 6.5	0.75- 2.0	-	2.0 - 3.0	-	0.10 - 0.35	min. 30	Min. 485

The characteristic of the alloy design of S82551 is to use Cu, instead of Mo, to ensure comparable corrosion resistance and strength. In addition, due to the significant decrease in Mo content, S82551 is expected to be less sensitive to sigma phase precipitation during single or multi-pass welding[4].
This work investigated the effect of weld thermal cycling on sigma phase precipitation behaviour in S82551 welds comparing with S31803 and S32750.

Experimental method

Material

The material used for this research was laboratory melted duplex stainless steel plates with chemical composition of S82551, S31803 and S32750. The plates (PM1, PM2 and PM3) were melted with a laboratory electric furnace and were fabricated to the 15mm thick plates by hot forging and hot rolling followed by 1100°C solution treatment followed by water quenching.

Table 1– Chemical composition of material investigated

Material	Mark	Chemical composition (mass%)							Notes
		C	Mn	Cu	Ni	Cr	Mo	N	
Plate	PM1	0.015	0.9	2.4	4.9	24.8	1.0	0.19	UNS S82551
	PM2	0.015	1.2	0.3	5.2	22.9	3.2	0.18	UNS S31803
	PM3	0.015	0.7	0.1	7.0	25.0	4.1	0.27	UNS S32750

Multiple thermal cycling simulation of lower temperature HAZ at 900°C was performed to investigate the effect of the cooling rate and the number of thermal cycles on the formation of sigma phase.

Table 2– Test condition for thermal cycling test

Material	Heating rate	Peak temp.	Holding time	Cooling rate	Cycles
PM1 (UNS S82551)	80°C/s	900°C	3s	30°C/s	1,3,5,7,9
			5s	5°C/s	
			10s	3°C/s	
PM2 (UNS S31803)	80°C/s	900°C	3s	30°C/s	1,3,5,7,9
			5s	5°C/s	
			10s	3°C/s	
PM3 (UNS S32750)	80°C/s	900°C	3s	30°C/s	1,3,5,7,9
			5s	5°C/s	
			10s	3°C/s	

Results and analysis

Ferrite content after thermal cycling

It is basically known that ferrite phase transformation into sigma phase and secondary austenite by long holding time with high temperature such as multiple thermal cycling during welding with higher heat input. Therefore, it is important to evaluate the ferrite content in tested material before transforming into sigma phase, which has relationship with the area fraction of sigma phase precipitation.
Fig.1 shows the ferrite content in PM1, PM2 and PM3 after thermal cycling did not show a significant change with increasing the number of cycles.

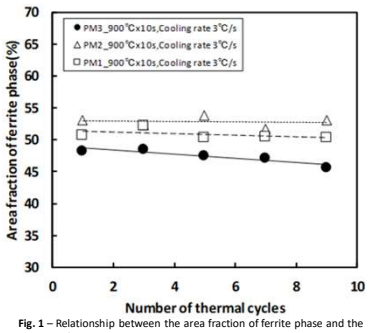

Fig. 1 – Relationship between the area fraction of ferrite phase and the number of thermal cycles

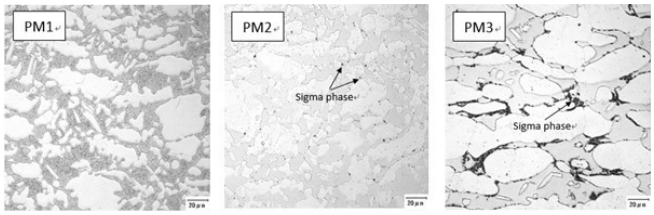

Fig. 2 – Microstructure of PM1, PM2 and PM3 after thermal cycle test (900°C x 10s → 3°C/s x 9cycles)

Results and analysis

Sigma phase precipitation

As shown in Fig. 2, for PM1, sigma phase was not observed for any condition even after 9 thermal cycles applied. For PM2, the small amounts of sigma phase were observed at α/γ grain boundaries. For PM3, sigma phase was clearly observed.
Fig. 3 shows the effect of the number of thermal cycles on the amount of the sigma phase for PM1, PM2 and PM3. The amount of sigma phase increases with the number of thermal cycles for PM2 and PM3, however, for PM1, sigma phase precipitation was not observed even when the combination of lowest cooling rate (3°C/s) and highest thermal cycles (9 cycles) was employed.

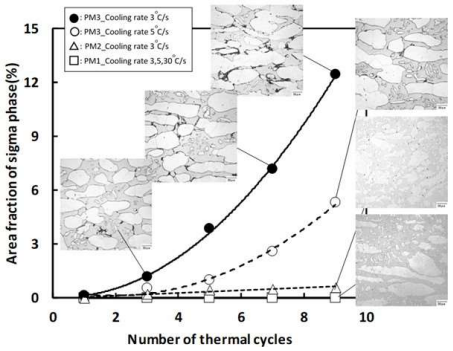

Fig. 3 – Relationship between the area fraction of sigma phase and the number of thermal cycles

Isothermal kinetics of sigma phase precipitation

It was reported that the growth of sigma phase accords to the JMAK equation[5,6].

$$X = 1 - \exp\left[-\frac{V_{ex}}{V_0\omega}\right] = 1 - \exp[-(kpt)^m] \text{ (m = 5/2)} \cdots (1)$$

Growth rate constant $k_p = K_\infty \left(\frac{T_{eq}}{\Delta T}\right)^{4/5} D_{eff} exp\left(-\frac{\Delta G_h}{RT}\right)$ ・・・(2)

$$K_\infty = [(16\sqrt{2}\pi^2/15V_0 \cdot C_0 N_0 \omega^{\frac{1}{2}}\sigma^2/(C_p\Delta H)^2/r_\alpha^4)]^{2/5} \cdots (3)$$

$$\Delta G_h = \varphi(T_{eq}/\Delta T)^2 \cdots (4)$$

$$\varphi = 32\pi/15V_0^2 N_0 \cdot \sigma^3/(C_p\Delta H)^2 \cdots (5)$$

V_0 : Volume of sigma phase, **C_0** : Concentration of dominant atom to determine the growth rate, **N_0** : Number of atom, **ω** : Supersaturation, **σ** : interface energy, **C_p** : Concentration in sigma phase of dominant atom to determine the growth rate, **ΔH** : Enthalpy of transformation, **r_a** : lattice constant **T_{eq}** : Equilibrium solvus temperature of sigma phase, **ΔT** : Degree of undercooling (=T_{eq}-T)

Applying the additivity rule, each progress ratio of precipitation X in the continuous cooling process for Δt at T_i is shown as follows,

$$[-\ln(1-X_i)]^{1/n} = ([-\ln(1-X_{i-1})]^{1/n} + k_p(T_i)\Delta t) \cdots (6)$$

The amount of the sigma phase precipitated during the arbitrary thermal cycle is calculated by Eq. (7):

$$X = 1 - \exp[-(\textstyle\sum_{i=1}^{m} k_p(T_i)\Delta t)^n] \quad \text{(n=5/2)} \cdots (7)$$

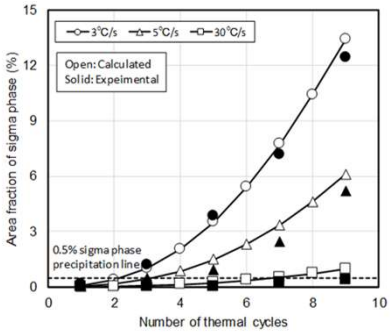

Fig. 4 – Prediction of the area fraction of sigma phase for PM3 during weld thermal cycles

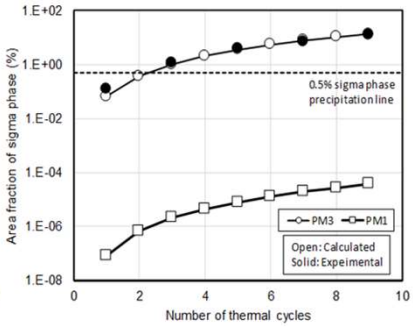

Fig. 5 – Comparison of the area fraction of sigma phase between PM1 and PM3 after thermal cycles

Discussions and Conclusions

It can be concluded that:

- During thermal cycling in the experimental work and the calculation, the amount of sigma phase increased with increasing the number of thermal cycles, and lower cooling rate for UNS S31803 and UNS S32750, but sigma phase was not observed for new alloy UNS S82551.
- Based on the isothermal kinetics of sigma phase precipitation, the amount of sigma phase precipitated during thermal cycle can be predicted by applying the additivity rule to the physical model. The area fractions of sigma phase calculated have a good fit to the experimental ones.
- The new steel UNS S82551 has less sensitivity to sigma (s) phase precipitation during multi-pass welding than conventional UNS S31803 and UNS S32750 mainly because of lower Mo content.

References

1. D. Motoya, K. Yamada, S. Nakatsuka, H. Takabe, M. Hamada, H. Amaya, M. Ueda, M. Sagara and K. Ogawa, Eurocorr. 2012, European Federation of Corrosion, (2012).
2. M. Sagara, A. Nishimura, S. Nakatsuka, K. Yamada, D. Motoya, H. Takabe, H. Amaya, K. Ogawa and M. Ueda, Corrosion/2013, Paper No.2561, NACE International, TX (2013).
3. M. Sagara, A. Nishimura, J. Nakamura, H. Shitamoto, K. Yamada, D. Motoya, H. Takabe, H. Amaya, K. Ogawa and M. Ueda, Corrosion/2015, Paper No.5703, NACE International, TX (2015).
4. K. Yamada, T. Osuki, K. Ogawa, B. Holmes, K. Sotoudeh and H. Dong, ISIJ International, 63 (2023) 143-149.
5. K. Ogawa and T. Osuki, ISIJ International, 59 (2019) 122-128.
6. K. Ogawa and T. Osuki, ISIJ International, 59 (2019) 129-135.

EPSRC Engineering and Physical Sciences Research Council
UNIVERSITY OF LEICESTER
UNIVERSITY OF BIRMINGHAM
The University of Nottingham UNITED KINGDOM · CHINA · MALAYSIA